Plasma irradiation experiment on the metal pebble flow in the TPDsheet-U

Plasma Irradiation Experiment on the Metal Pebble Flow in the TPDsheet-U

Takeru Ohgo[a*], Takuya Goto[a,b], Toshikio Takimoto[c], Akira Tonegawa[c], Junichi Miyazawa[a,b]

[a]*The Graduate University for Advanced Studies, 322-6 Oroshi, Toki, Gifu 509-5292, Japan*
[b]*National Institute for Fusion Science, 322-6 Oroshi, Toki, Gifu 509-5292, Japan*
[c]*Tokai University, 4-1-1 Kitakaname, Hiratsuka, Kanagawa 259-1207, Japan*

A new divertor concept REVOLVER-D2 that uses metal pebbles as a divertor target has been proposed for the LHD-type helical fusion reactor FFHR-c1. Demonstration of sufficient plasma shielding rate is one of the important issues to show the feasibility of the REVOLVER-D2. For this purpose, an experiment on the plasma irradiation to the metal pebble flow has been conducted in the sheet plasma device TPDsheet-U in Tokai University. Reduction of the ion flux and electron density in the metal pebble flow was observed and it was confirmed that the metal pebble flow can play the role of the divertor target. The measured shielding rate is consistent with the prediction by the model based on the Lambert-Beer-Bouger's law. Achievement of the shielding rate of > 72 % is expected in the FFHR-c1 using the nozzle with the size of > 310 mm × 310 mm and the pebble flow with the diameter of 5 mm.

Keywords: divertor, metal pebble divertor, plasma irradiation, TPDsheet-U, shielding rate

1. Introduction

Removal of the heat load of several tens of MW/m^2 is one of the most important requirements on the divertor of a nuclear fusion reactor. This heat load is larger than the tolerable level of the conventional divertor with a solid target developed for ITER [1]. In the case of the helical fusion reactor FFHR-c1 [2], which is the heliotron-type reactor based on the Large Helical Device (LHD), the estimated maximum heat load on the divertor plate is ~40 MW/m^2. In the case of a commercial reactor, the heat load increases further. To satisfy the requirements on the divertor, various "renewable" divertor concepts have been proposed. In T3-M tokamak, gallium limiters of droplet stream and film flow were tested [3]. In T11-M tokamak, experiments with lithium Capillary Pore Systems (CPS) were conducted [3]. Similar lithium limiters have been tested in several devices including CDX-U, FTU, and TJ-II [4-6]. The use of a liquid metal flow for a wall protection is also considered in IFE devices, such as HYLIFE [7] and KOYO-F [8]. In the conceptual design of FFHR-c1, the ergodic limiter/divertor REVOLVER-D, which consists of the shower of molten tin jets, has been proposed. The REVOLVER-D is expected to accommodate the heat load of a few tens of MW/m^2 by using a high speed continuous flow of molten tin [9]. The liquid metal shower units are placed at the inboard side of the torus of the 10 sections where the plasma has a horizontally-elongated cross-section and jets are inserted into the so-called ergodic region surrounding the main plasma. The plasma particles flowing out from the main plasma to the ergodic region are neutralized when the plasma particles collide with the jets and the heat flux that originally goes to the helical divertor is mitigated. Because the neutralized particles can be pumped out through the gaps of the shower, a high evacuation efficiency can be expected. To estimate the reduction of particle and heat flux to the original helical divertor, the numerical simulation of the particle tracking using the three-dimensional edge transport code EMC3-EIRENE has been carried out with the condition of the LHD [10]. The liquid metal shower forms the shape of a square pillar. It was estimated that more than 80% of the heat and particle flux to the original helical divertor can be mitigated if the limiter covers the entire region and has 100% shielding efficiency against the plasma particles. However, it has been found that the deformation of the liquid metal jet by the Lorentz force due to the electric current induced by the plasma and the existing magnetic field will be an unacceptable level in the reactor condition [11].

If a pebble flow is selected as the renewable divertor

*present affiliation and address: Nippon Advanced Technology Co. Ltd., 3129-45 Hibara Muramatsu, Tokai, Ibaraki 319-1112, Japan

target instead of liquid metal jets, there is no current path along the flow. In past studies, applicability of multi-layered ceramic pebbles as the divertor target has been investigated [12, 13]. In this study, 100% shielding rate was achieved by the ceramic pebbles with a diameter of 1 mm [12]. However, collection of broken pebbles and replenishment of new pebbles in a continuous circulation are important issues if ceramic pebbles are to be used as the divertor target. The size of pebbles is limited due to the thermal stress. To solve the issues of the REVOLVER-D and the ceramic pebble divertor, a new renewable divertor concept REVOLVER-D2, which uses the flow of fusible metal pebbles instead of the liquid metal jet of the REVOLVER-D, has been proposed [14]. The use of a metal pebble divertor has also been proposed by the FZJ group [15]. In the concept of the fusible metal pebbles, the pebbles can be melted and remanufactured during the circulation.

In the previous study on the ceramic pebble divertor, irradiation experiments of the ceramic pebble by electron beam and neutral beam have been carried out to investigate temperature increase, corruption, and corrosion of the ceramic pebble [16]. However, plasma irradiation to the pebble flow has not been conducted yet. The plasma shielding characteristics of the pebble flow must be examined. This paper describes the experimental results of the plasma irradiation to the metal pebble flow. The analytical model for the estimation of the shielding rate of the pebble flow is described in Section 2. The experiment for the validation of the shielding rate model is described in Section 3. The experiment of the plasma irradiation to the metal pebble flow is described in Section 4. This plasma irradiation experiment was conducted by the sheet plasma device TPDsheet-U in Tokai University.

2. The shielding rate model

In the previous study of the ceramic pebble divertor, the shielding rate of the pebble flow was estimated by the model derived from the Lambert-Beer-Bouger's law [12]. In this study, this model is extended to arbitrary initial velocity and nozzle shape. The Lambert-Beer-Bouger's law describes the light intensity I after passing through the medium with the distance d:

$$I = I_0 \exp(-a_\lambda d) \dots (1),$$

where I_0 is the initial light intensity and a_λ is spectral absorption coefficient. Considering the flow of the pebbles

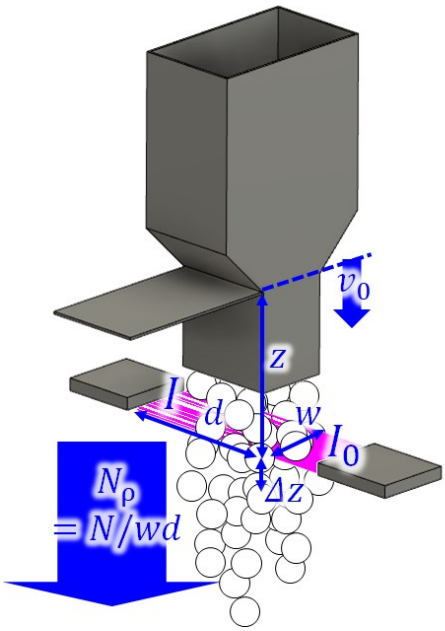

Figure 1 The model of the shielding rate by the pebble flow in the rectangle whose width : w, depth : w, height : Δz.

with a diameter of r, the spectral absorption coefficient is given by:

$$a_\lambda = \pi r^2 n e_\lambda \dots (2),$$

where πr^2 is the projected area of the pebble, n is the number density of the pebble in the measurement region, and e_λ is spectral absorption efficiency. Here we assume that the plasma particle completely loses its energy when it collides with the pebble, i.e., $e_\lambda = 1$.

Considering the pebble flow with the width of w and the depth of d as shown in Fig. 1, n is given by

$$n = \frac{N\Delta t}{wd\Delta z} \dots (3),$$

where N is the number flow rate of the pebble flow, Δz is the drop distance in Δt. Δt is given by

$$\Delta t = \frac{\sqrt{v_0^2 + 2g(z+\Delta z)} - \sqrt{v_0^2 + 2gz}}{g} \dots (4),$$

where v_0 is the initial velocity of the pebble flow, z is the drop distance, and g is the gravitational acceleration.

Substituting Eqs. (2)–(4) into Eq. (1), the shielding rate by the pebble flow SR is given by

$$SR = 1 - \frac{I}{I_0} = 1 - \exp\left(-\frac{2\pi r^2 N}{w}\frac{1}{\sqrt{v_0^2 + 2g(z+\Delta z)} + \sqrt{v_0^2 + 2gz}}\right) \quad \ldots (5)$$

In the experiment, $N \propto wd$ if the nozzle is large enough. Defining $N_\rho = N/wd$ as the number flow rate per unit area, Eq. (5) can be transformed into

$$SR = 1 - \exp\left(-\frac{2\pi r^2 N_\rho d}{\sqrt{v_0^2 + 2g(z+\Delta z)} + \sqrt{v_0^2 + 2gz}}\right) \quad \ldots (6).$$

In the actual condition, overlap of the pebbles will occur and the effective shielding rate is decreased. Then the spectral absorption coefficient in Eq. (2) gives the achievable maximum value.

Consequently, the shielding rate depends on the pebble radius r, the number flow rate of the pebble flow per unit area N_ρ, the depth of the pebble flow region d, and the drop distance z. In this study, Δz is given as the pebble diameter $2r$.

In the previous study, the experiment for the validation of the model was conducted. The experimental result agrees very well with the model prediction and 100% shielding rate was achieved by adjusting the nozzle width [12]. However, the experiment was conducted in the limited condition: the pebble radius is 0.5 mm and the vertical distance between the nozzle and the measurement device of 500 mm. In the REVOLVER-D2 for the FFHR-c1, the pebble radius of 2.5 mm and the drop distance of 5,000 mm are considered. The number flow rate of the pebbles is proportional to $1/r^3$ if a volume flow rate is constant. According to Eq. (5), the decrease of the shielding rate with decreasing the number flow rate can be compensated by the increase of the depth of the pebble flow. However, this effect must be examined by an experiment.

3. Validation experiment of the model

To investigate the dependence of the shielding rate of the pebble flow on the pebble radius, volume flow rate and the drop distance, experimental measurement of the shielding rate has been carried out. The experimental setup is described in Fig. 2. The shielding rate is measured by the transmittance of a laser light. The shielding rates in different d (30, 40, 50 mm) and z (80–300 mm) were measured. Commercially available aluminum pebbles (density: 3,600 kg/m^3) with a diameter of 5 mm were used for this experiment. The total mass of the pebbles are ~0.95 kg (d = 30 mm), ~1.24 kg (d = 40 mm) and ~1.60 kg (d = 50 mm), respectively. A through-beam type laser detection sensor (KEYENCE IB-30) which produces sheet-shaped laser with the width of 30 mm was used for the measurement. The time resolution of the measurement device is 1/2000 s. The wavelength of the laser is 660 nm. Two sensors were placed at different heights.

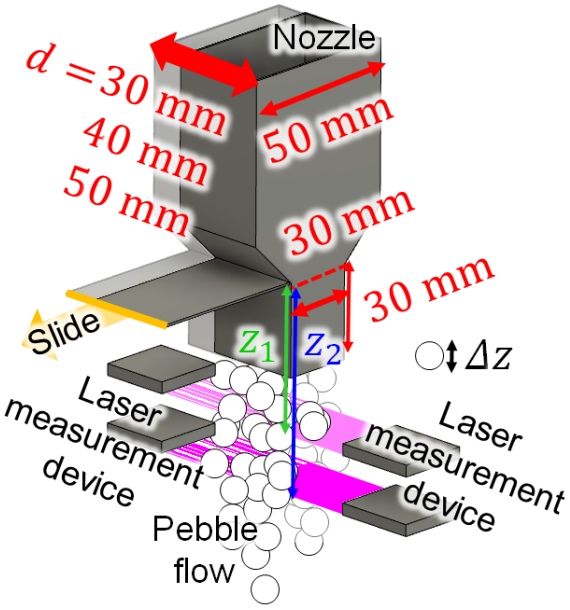

Figure 2 The experimental system of the shielding rate of the pebble flow.

Figure 3 shows the comparison of the experimentally measured shielding rate and that predicted by the shielding rate model (Eq. (6)). According to the measurement by a fast camera, the initial velocity of the pebble flow and the number flow rate of the pebbles in per unit area N_ρ are estimated to be ~0.36 m/s and ~3.8×10^6 m^{-2}s^{-1}, respectively. The shielding rate decreases with increasing the drop distance z and decreasing the depth of the pebble flow region d as the prediction by the model. However, experimentally obtained shielding rates were lower than the model prediction in all cases. The difference between the experimental result and the model prediction increases with increasing the drop distance z.

In this experiment, the width of the laser light (30 mm)

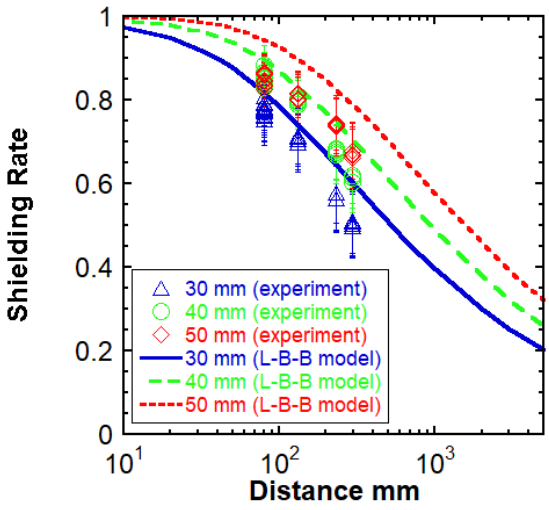

Figure 3 Experimental results of the shielding rate by the pebble flow (△ : $d = 30$ mm, ○ : $d = 40$ mm, ◇ : $d = 50$ mm). The equation of the shielding rate model (solid line : $d = 30$ mm, long broken line : $d = 40$ mm, broken line : $d = 50$ mm).

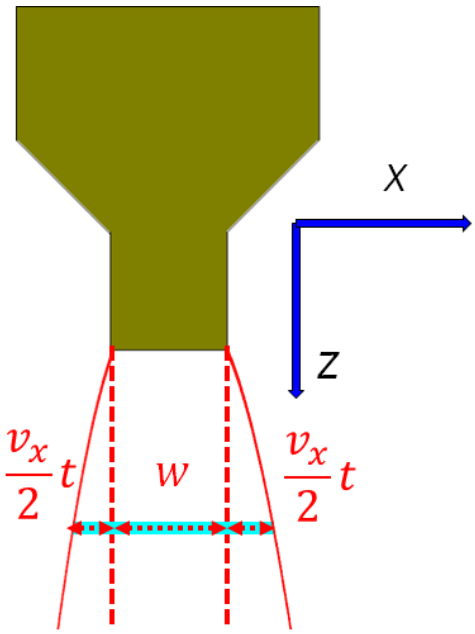

Figure 4 The pebble scattering model.

was just the same as the nozzle width. This means that the number of the pebbles in the measurement region decreases with the drop distance if the pebbles have a finite velocity with the horizontal direction. To take this effect into account, the scattering of the pebble flow region with a constant horizontal velocity v_x is assumed as shown in Fig. 4. The drop distance z and the scattering width of the pebble flow x as a function of time t are described as

$$z = \frac{1}{2}gt^2 + v_0 t \ldots (7),$$

$$t = \frac{-v_0 + \sqrt{v_0 + 2gz}}{g} \ldots (8),$$

$$x = v_x t \ldots (9).$$

Assuming a constant number density of the pebble flow, the number flow rate of the pebbles with considering the pebble scattering N_{rem} can be described as

$$N_{\mathrm{rem}} = N\frac{w}{w + x} \ldots (10).$$

where N is the initial number flow rate of the pebble flow (at t = 0). Then, the shielding rate with a consideration of the pebble scattering effect is obtained by replacing N in Eq. (5) with N_{rem} in Eq. (10). The comparison of the experimental result with the prediction by the modified model is shown in Fig. 5. The results agree well with the model prediction in the case of v_x = 0.05 m/s. This value corresponds to the horizontal velocity of the pebbles estimated from the measurement by the fast camera.

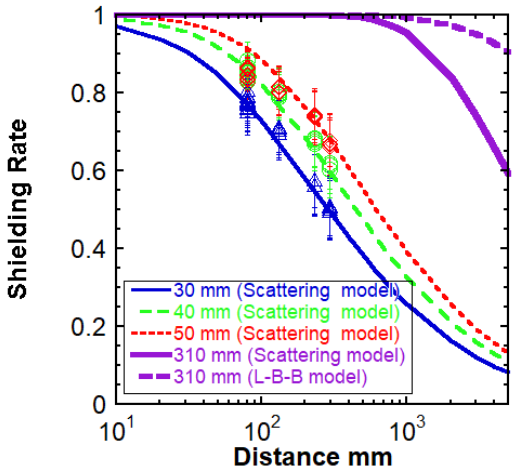

Figure 5 Experimental results of the shielding rate by the pebble flow (△ : $d = 30$ mm, ○ : $d = 40$ mm, ◇ : $d = 50$ mm). The equation of the shielding rate model considering the pebble scattering (solid line : $d = 30$ mm, long broken line : $d = 40$ mm, broken line : $d = 50$ mm, thick solid line : 310 mm, thick solid line : 310 mm, (no pebble scattering)).

Consequently, it has been confirmed that the shielding rate model based on the Lambert-Beer-Bouger's law is applicable to the various pebble radii and drop distances if the pebble scattering effect is taken into account.

Assuming that the number flow rate in per unit area N_ρ in FFHR-c1 is the same as that in the experiment, the required pebble flow depth d for FFHR-c1 can be estimated. The calculation result is also plotted in Fig. 5. As described in the previous section, the drop distance in FFHR-c1 is estimated to be 5,000 mm. Without the pebble scattering, the shielding rate of 90% can be achieved in the case of d = 310 mm. However, the shielding rate decreases to 60% if the pebble scattering with the same horizontal velocity (v_x = 0.05 m/s) is assumed. Therefore, the mitigation of the pebble scattering is desired in a certain way, such as an optimization of the nozzle shape.

As described in the Section 2, reduction of the heat flux to the original helical divertor by a "perfect" wall is ~80%. Thus, the REVOLVER-D2 in FFHR-c1 can mitigate ~72% of the heat load to the original helical divertor. However, this estimation is simply based on the attenuation of the laser intensity by the pebble flow. Therefore, investigation of the plasma shielding characteristic of the pebble flow is necessary.

4. Plasma irradiation experiment

To examine the plasma shielding effect of the pebble flow, an experiment on the plasma irradiation to the metal pebble flow was conducted in the sheet plasma device TPDsheet-U in Tokai University. The TPDsheet-U is a linear plasma device [17]. The sheet plasma is generated in the linear magnetic field generated by the solenoid coils. The maximum magnetic field, electron temperature and electron density in the plasma confinement region are ~0.12T, ~20 eV and ~1×10^{19} m^{-3}, respectively. The thickness of the sheet plasma is ~10 mm. In this experiment, hydrogen was used as a working gas.

Figure 6 shows the schematic view of the plasma irradiation experiment. The pebble falling device with two gate valves and one ball valve was attached on the upper and the lower ports of the TPDsheet-U. The sequence of the plasma irradiation experiment is shown as below.

1) Close both gate valves and evacuate the main chamber.
2) After closing the ball valve, open the top blank flange and insert the pebbles.
3) Close the top lid and evacuate the sub-chamber.
4) Open both gate valves.
5) Open the ball valve and drop the pebbles.
6) After all pebbles are dropped into the removable vessel, close all valves and vent the sub chamber and the removable vessel.
7) Unmount the removable vessel and collect pebbles.

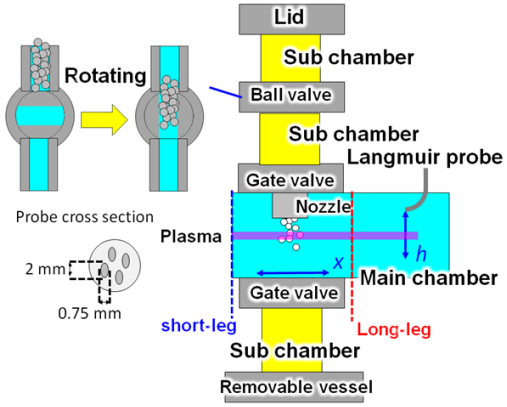

Figure 6 The schematic view of the plasma irradiation experiment.

The sequence from 2) to 7) was repeated if necessary. While the pebbles are falling, the plasma diagnostics by a Langmuir probe and the video recording by a fast video camera were conducted. The Langmuir probe was placed at the plasma downstream behind the pebble flow. The Langmuir probe was moved over the range of h = −20 to 20 mm in the vertical direction (h = 0 is the position of the peak of the plasma center) to obtain the plasma profile. The voltage of the probe was swept from −97 to 87 V with the frequency of 100 Hz. In this experiment, the pebbles made of U-alloy78 ($Bi_{57}In_{17}Sn_{26}$ with the melting point of 78°C) with a diameter of 3 mm were used. The diameter of the nozzle is 23 mm.

Figure 7 shows the photo of the plasma with the pebble flow taken by a high-speed camera. The attenuation of the plasma by the pebble flow was visually observed. Figure 8 shows the V-I characteristic of the plasma without the pebble flow at h = 0 (solid line), without the pebble flow at h = ±20 (long broken line), with pebble flow at h = 0 (short broken line), and with pebble flow at h = ±20 (dotted line). The ion saturation current $I_{i,\mathrm{sat}}$ is obtained as the average of the current in the voltage range from −70 to −50 V. The electron saturation current $I_{e,\mathrm{sat}}$ is obtained as the average of the current in the voltage range from 50 to 70 V. The electron temperature T_e is obtained by

$$T_e = \frac{e}{k_B}\frac{1}{\frac{\mathrm{d}\ln(I)}{\mathrm{d}V}} \quad \ldots (11).$$

Figure 7 The photo of the plasma with the pebble flow taken by a high-speed camera (shutter speed: 1/1,000 sec). The left side of the photo corresponds to the plasma upstream.

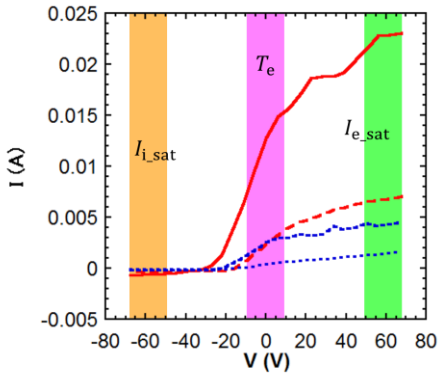

Figure 8 The *V*-*I* characteristic of the plasma during no pebble flow at $h = 0$ (solid line), no pebble flow at $h = \pm 20$ (long broken line), pebble flowing at $h = 0$ (short broken line), and pebble flowing at $h = \pm 20$ (dotted line).

where e = 1.602×10^{-19} C and k_B = 1.381×10^{-23} J/K are the elementary charge and the Boltzmann constant, respectively. $\mathrm{d}\ln(I)/\mathrm{d}V$ is obtained using the five data points in the voltage range from −10 to 10 V by the least square method. The ion flux Γ_i given by

$$\Gamma_i = \frac{I_{i,\mathrm{sat}}}{eS} \ldots (12),$$

where S = 4.71×10^{-6} m^2 is the probe cross section. The electron density n_e given by

$$n_e = \frac{I_{e,\mathrm{sat}}}{eS\sqrt{\frac{8k_BT_e}{\pi m_e}}} \ldots (13),$$

where m_e = 9.11×10^{-31} kg is the electron mass. The triangle and circle symbols correspond to the data with and without pebble flow, respectively.

The profiles of electron temperature, ion flux and electron density are shown in Figs. 9–11. Without the pebble flow, the peak electron temperature, the peak ion flux and the peak electron density were ~25 eV, ~2.5×10^{21} m^{-2}s^{-1} and ~3.7×10^{16} m^{-3}, respectively. With the pebble flow, the peak ion flux and the peak electron density decreased to ~1.0×10^{21} m^{-2}s^{-1} and ~1.1×10^{16} m^{-3}, respectively. The attenuation rate of the ion flux and electron density at the peak position (h = −5 to 5 mm) were 77±4% and 86±1%, respectively. The electron temperature with the pebble flow was scattered and it is difficult to measure the effects of the pebble flow on the electron temperature. At the least, there is no clear evidence of the attenuation of the electron temperature.

According to the shielding model based on the Lambert-Beer-Bouger's law shown in the section 2, the shielding rate in this experiment is estimated to be 74%. The parameters used in the estimation are as follows. The initial velocity is $v_0 = 1.2$ m/s, the drop distance is 20 mm, the pebble flow width and depth are 23 mm (same as the diameter of the nozzle), the number flow rate of the pebble flow in per unit area N_ρ was ~1.2×10^7 m^{-2}s^{-1}, and the pebble horizontal velocity v_x = 0.05 m/s. The shielding rate estimated by this model includes the error in the measurement of the ion flux. The heat load on the divertor can be evaluated as the product of the ion flux and the plasma temperature. Consequently, it was successfully demonstrated that the pebble flow can mitigate the heat load to the original helical divertor. However, the reduction of the electron temperature is desired from the viewpoint of the suppression of the erosion of the divertor plate by the physical sputtering. Combination with a gas puffing may be a solution to this issue.

The electron density in this experiment (~3.7×10^{16} m^{-3}) was much lower than that in a reactor condition. The pebbles in the plasma can be charged up. According to the estimation by a simple 1D sheath model, the charge on the

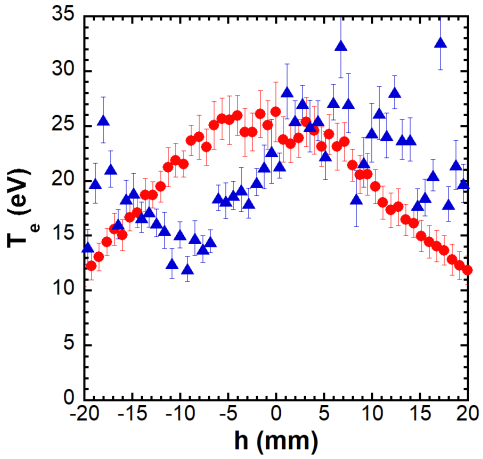

Figure 9 The electron temperature in the case of the pebble flowing (the triangle symbol ▲) and no pebble flow (the circle symbol ●).

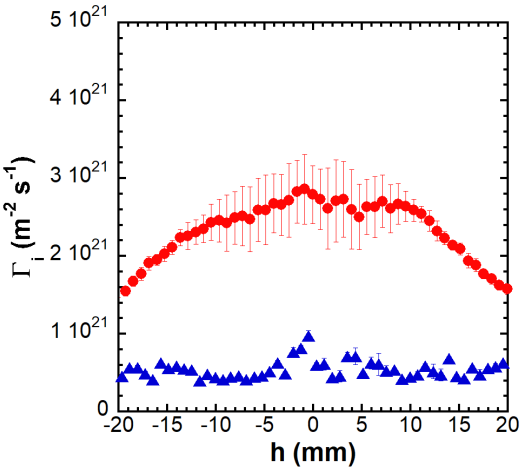

Figure 10 The ion flux in the case of the pebble flowing (the triangle symbol ▲) and no pebble flow (the circle symbol ●).

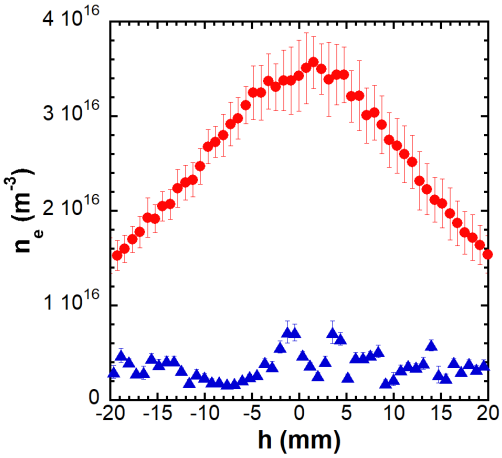

Figure 11 The electron density in the case of the pebble flowing (the triangle symbol ▲) and no pebble flow (the circle symbol ●).

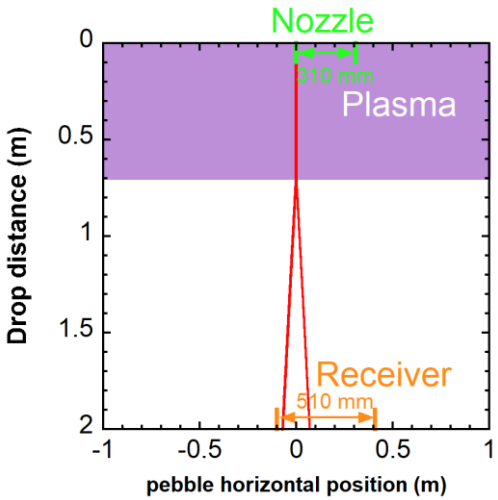

Figure 12 Trajectory of the two pebbles issued at the edge of the nozzle in the condition of FFHR-c1.

pebble will be the order of 10^{-8} C in the case of FFHR-c1 with the assumption that the electron density and the electron temperature in the ergodic region are 1.0×10^{19} m^{-3} and 200 eV, respectively. Figure 12 shows the calculation result of the trajectory of the two pebbles with the diameter of d = 5 mm which have the charge of 10^{-8} C and initially contact each other. The velocity of the pebbles at the drop distance of 0 m is set to be 10 m/s. If the space between the two pebbles is less than 2d, the Coulomb force between the two pebbles exceeds the gravity force on each pebble (The magnitudes of these forces are the order of 10^{-2} N. The Lorentz force is the order of 10^{-6} N and negligible.) In this calculation, it is assumed that the Coulomb force does not act in the plasma region because of the Debye shielding effect. At the position of pebble receiver (the drop distance of 2 m), the distance of the two pebbles increases to 140 mm. In the case of FFHR-c1, a square nozzle shape with 310 mm sides is assumed. Therefore, this scattering can be dealt with the square receiver with the sides of ~510 mm and there is enough space to place the receiver of this size. Because this estimation is based on a quite simple assumption, a similar plasma irradiation experiment with the higher electron density, the lighter pebbles and the pebble flow with the higher number density is required [18] to closely investigate this effect of the Coulomb force.

5. Conclusion

In order to examine the applicability of the flow of the metal pebbles as a divertor target of a fusion reactor, the plasma irradiation experiment on the pebble flow was conducted in the sheet plasma device, TPDsheet-U. The

model for the estimation of the shielding rate of the pebble flow, which was developed in the previous study, has been extended to arbitrary initial velocity and nozzle shape. This extended model has been validated by the experiment and it is confirmed that the model is applicable to various pebble radii and the different drop distances. It is predicted that the attenuation of the heat load on the original helical divertor by 72% can be achieved in the condition of the helical fusion reactor FFHR-c1 with the pebble diameter of 5 mm and the drop distance of 5 m.

Some issues remain to be solved to realize the pebble divertor concept. One of the important issues is the effect of impurities generated by the interaction between the plasma and the pebbles in the main plasma and the original divertor. Regarding the effect on the main plasma, good impurity screening in the ergodic layer has been observed in the LHD experiment [19]. This result indicates that the friction force that causes downstream flow increases with the increasing density. Therefore, main plasma impurity contamination is expected to be avoided in reactors with high electron density. Regarding the effect on the original divertor, examination in small-scale experiments is required. Although there are some other issues that are mentioned in this paper (reduction of the electron temperature, interaction between the plasma and pebbles in a high heat load condition and behavior of the charged pebbles), it was successfully confirmed that the flow of the metal pebbles can work as a divertor target and mitigate the heat load on the original divertor.

Acknowledgments

This work is supported by the budget NIFS10UFFF038 of National Institute for Fusion Science. The authors also appreciate the members of the Fusion Engineering Research Project in NIFS for providing valuable comments and advice.

References

[1] J. Schlosser, et al., Technologies for ITER divertor vertical target plasma facing components, Nucl. Fusion **45** (2005) 512.

[2] J. Miyazawa, et al., Maintainability of the helical reactor FFHR-c1 equipped with the liquid metal divertor and cartridge-type blankets, Fusion Eng. Des. **136** (2018) 1278.

[3] S.V. Mirnov and V.A. Evtikhin, The Use of Liquid Ga and Li as Limiter Material in T-3M and T-11M Tokamaks, Fusion Sci. Technol. **47** (2005) 698.

[4] S. Mirnov, Plasma-wall interactions and plasma behaviour in fusion devices with liquid lithium plasma facing components, J. Nucl. Mater. **390** (2009) 876.

[5] G. Mazzitelli, et al., Heat loads on FTU liquid lithium limiter, Fusion Eng. Des. **86** (2011) 580.

[6] F.L. Tabarés, et al., First liquid lithium limiter biasing experiments in the TJ-II stellarator, J. Nucl. Mater. **463** (2015) 1142.

[7] R.W. Moir, HYLIFE-II inertial confinement fusion power plant design, Part. Accel. **37-38** (1992) 467.

[8] T. Norimatsu, et al., Conceptual Design of Fast Ignition Power Plant KOYO-F Driven by Cooled Yb:YAG Ceramic Laser, Fusion Sci. Technol. **52** (2007) 893.

[9] J. Miyazawa, et al., Conceptual design of a liquid metal limiter/divertor system for the FFHR-d1, Fusion Eng. Des. **125** (2017) 227.

[10] G. Kawamura, et, al., "Application of EMC3-EIRENE to Estimation of Influence of a Liquid Metal Limiter on an LHD-Type Fusion Plasma", Plasma Fusion Res. **13** (2018) 3403034.

[11] T. Goto, et al., "Experimental Study on MHD Effect of Liquid Metal Sheath Jet for the Liquid Metal Divertor REVOLVER-D", Plasma Fusion Res. **14** (2019) 1405092.

[12] T. Okui, et al., Performance characteristics of pebble flow for pebble divertor, Fusion Eng. Des. **61-62** (2002) 203.

[13] M. Isobe, et al., Multilayer pebbles for application to new divertor systems, Nucl. Fusion **40** (2000) 327.

[14] T. Ohgo, et al., "A New Divertor System Using Fusible Metal Pebbles", Plasma Fusion Res. **14** (2019) 3405050

[15] N. Gierse, et al., Conceptual study of ferromagnetic pebbles for heat exhaust in fusion reactors with short power decay length, Nucl. Mater. Energy **2** (2015) 12-19.

[16] M. Isobe, et al., Irradiation experiments of divertor pebble s, Fusion Eng. Des. **49-50** (2000) 223.

[17] K. Hanai et al., Characteristics of cesium-free negative hydrogen/deuterium ion source by sheet plasma, Fusion Eng. Des. **146** (2019) 2721.

[18] T. Okui, et al., Behavior of Falling Pebble for Pebble Divertor, Fusion Sci. Tech. **934-938** (2001) 39.

[19] S. Morita, et al., Effective screening of iron impurities in the ergodic layer of the Large Helical Device with a metallic first wall, Nucl. Fusion **53** (2013) 093017.